Athens Institute for Education and Research
ATINER

ATINER's Conference Paper Series
ELE2017-2380

Considerations of the Experimental Verifications of the Numerical Model of a Permanent Magnet Synchronous Motor Mounted in the Wheel of an Electric Bicycle

Silvia-Maria Diga
Professor
University of Craiova
Romania

Leonardo-Geo Manescu
Professor
University of Craiova
Romania

Adelaida-Mihaela Duinea
Lecturer
University of Craiova
Romania

Nicolae Diga
PhD Design Engineer
University of Craiova
Romania

ATINER CONFERENCE PAPER SERIES No: ELE2017-2380

An Introduction to ATINER's Conference Paper Series

ATINER started to publish this conference papers series in 2012. It includes only the papers submitted for publication after they were presented at one of the conferences organized by our Institute every year. This paper has been peer reviewed by at least two academic members of ATINER.

Dr. Gregory T. Papanikos
President
Athens Institute for Education and Research

This paper should be cited as follows:

Diga, S. M., Manescu, L. G., Duinea, A. M. and Diga, N.(2018).**"Considerations ofthe Experimental Verifications of the Numerical Model of a Permanent Magnet Synchronous Motor Mounted in the Wheel of an Electric Bicycle",** Athens: ATINER'S Conference Paper Series, No: **ELE2017-2380.**

Athens Institute for Education and Research
8 Valaoritou Street, Kolonaki, 10671 Athens, Greece
Tel: + 30 210 3634210 Fax: + 30 210 3634209 Email: info@atiner.gr URL: www.atiner.gr
URL Conference Papers Series: www.atiner.gr/papers.htm

ISSN: 2241-2891
05/02/2018

Considerations ofthe Experimental Verifications of the Numerical Model of a Permanent Magnet Synchronous Motor Mounted in the Wheel of an Electric Bicycle

Silvia-Maria Diga

Leonardo-Geo Manescu

Adelaida-Mihaela Duinea

NicolaeDiga

Abstract

The authors studied the numerical models using 2D and 3D methods of finite elements and made numerical simulations for the original configuration of a permanent magnet synchronous motor used to drive an electric bicycle by using the specialized software "ANSYS Electromagnetics Low Frequency" (Maxwell 2D / 3D, RMxprt) - products of the ANSYS Inc. Company.In this paper,wepresent the results of the experimental verifications of the machine in a motor regime. In order to perform experimental verifications of the numerical model as a motor, a laboratory montage was used to measure all the required parameters, namely: the developed torque, the current absorbed by the motor per each phase, the input voltage and current of the controller, and the studied motor speed. All of these measurements were made at different speeds.Then they were studied comparatively based on operating characteristics obtained throughcomputation and experimentation respectively. Thesecharacteristics included: the mechanical characteristic, electromagnetic torque = f (speed), $M = f(n)$, for $U = U_N$ and a certain value of the transducer position angle β ($\beta = 90^0$); the characteristic useful torque = f (current), $M = f(I)$; the characteristic stator current = f (speed), $I_f = f(n)$.The authors also present an algorithm of construction by computation of the mechanical characteristic $M = f(n)$, for $U = U_N$ and a comparison between the mechanical characteristics obtained by computation, simulation and measurement in a permanent regime.

Keywords: Algorithm of Construction by Computation of the Mechanical Characteristic, Experimental Verifications, Mechanical Characteristic, Permanent Magnet Synchronous Motor.

Acknowledgments: First of all, the authors wish to express their special thanks and profound gratitude to Professor ConstantinGhiţă from the Department of Machines, Materials and Electric Drives of the Faculty of Electrical Engineering of POLITEHNICA University of Bucharest, for his direct and permanent contribution concretized in the careful and competent guidance made with his well-known exigency and rigor and the professional

support offered during the elaboration of the doctoral thesis (Diga, 2015) and other works regarding the study of synchronous machines with permanent magnets used in the electric drive systems of the bicycles.Also we should mention that the results presented in this research paper were obtained with the logistic support of S.C. INAS S.A. Craiova, Partnership - Collaboration Contract no. PC 1527 of 17.03.2014.Therefore the authors thank and express their complete gratitude to the Board of Directors of S.C. INAS S.A. Craiova, a Romanian representative of ANSYS Inc., a licensee of the CAD/CAM/CAE software solutions distributor, who through General Manager ConstantinCiolofan allowed them access to advanced technologies and equipment by providing support hardware and software ANSYS Electromagnetics Low Frequency (Maxwell 2D/3D, RMxprt) - products of ANSYS Inc. He directly supported them in developing a wide range of applications, thus making it possible to functionally and constructively optimize the permanent magnet synchronous motor for driving a bicycle, which was the object of further studies on this research topic.

Introduction

At present, developments of new, efficient and non-polluting means of transport areincreasingly being sought.Thishas increased the interest in electric vehicles,thehistory of which is more or less old, but the technological level of which has not yet allowed current and widespread exploitation.

Most researchers agree that moving to vehicles equipped with electric motors in urban transport would lead to a significant decrease in pollution, as well as primary energy consumption. Thus, comparisons, even in terms of efficiency alone, areclearly favourable to electric vehicles overclassical ones. An electric vehicle operates at a efficiency of about 46% (from the energy stored in the vehicle accumulators, 46% is transmitted to the engine wheels as useableenergy) compared to internal combustion engines with a efficiency of only 18% (from the total energy stored in the tank of the internal combustion engine vehicle, only approximately 18% is transmitted to the engine as useableenergy).

The current state of development of unconventional electric vehicles, which will massively take place in the transport of people, includestheir use as scooters, electric bicycles, electric vehicles for proximity transport, electric carts, or tiny propulsion kits for assisting electric wheelchairs, etc.

Some Examples of Electric Bicycles

In Table 1,wecomparatively analyse the technical characteristics of modern electric bicycles made by the same American manufacturer, Electric Vehicles Northwest, Inc. (http://www.gemcar.com), whose photos are shown in Figure 1:

a) LAfree Sport E-hybridis a modern electric bicycle incorporating speed and torque sensors, pedal activation system, Al frame, variable power control (VPC), providing good guidance and easy maintenance. The electric motor has a power of 400 W / 1000 W - peak load and the 7-speed can provide a good running even under relatively steep slopes. The VPC allows modification of the electric motor power / pedal power ratio, matching the power delivered to the pedals and the power output from the motor. The construction and materials used make this bicycle durable and yield good manoeuvrability, balance and easy maintenance.

b) Lite E-hybridis a hybrid electric bicycle with special qualities in terms of quietness, possessing active pedal system and providing a high torque and providing a value-adjustable speed of 30.5 km/h.Although the motor power is 240 W, the bicycle offers to the 400-500 W comparable performance bicycles, due to its efficient construction and low weight.

c) Joe-Fly Electric Bike is a bicycle that comes close to the design of mopeds or motorcycles. Still it preserved the features of the previous models, being lightweight and easy to handle. Suspensions on thewheels, efficient brakes, and used materials make it a very comfortable and safe electric bicycle. Although the motor power is 250 W, the bicycle provides a good speed adjustment range.

Table 1. *Technical Characteristics of Electric BicyclesType Electric Vehicles Northwest,* (http://www.gemcar.com)

Characteristics	LAfree Sport E-hybrid	Lite E-hybrid	Joe-Fly Electric Bike
Motor	24 V x 400 W – DC motor	12 V x 240 W – DC motor	36 V x 250 W - DC motor with permanent magnets, placed on the front wheel axle
Battery	2 x 12 V; 12 Ah - Yuasa	12 V x 6 Ah - fast charge NiMH	36 V x 5 Ah
Speed [km/h]	> 24	30.5	> 24
	variable adjustable speed (7 steps)	variable adjustable speed	variable adjustable speed (gearshift: rear - 5 steps)
Maximum load supported [kg]	25		
Total weight [kg]	22 (with batteries)	22 (with batteries)	32 kg (without batteries)
Price [$]	995	1145	1895

A pilot factory located in the Industrial Park of Craiova (https://e-twow.ro), nearby Oltenia region in Romania, which had started tooperate in the second half of 2015 supported by a European finding, produces small electric vehicles on two wheels, from mini scooters and electric bicycles up to larger scooters (1.5 kW and 3 kW) and electric wheelchairs.

Figure 1. *Electric Bicycles Variants, Electric Vehicles Northwest, Inc. USA: a) - LAfree Sport E-hybrid; b) - Lite E-hybrid; c) - Joe-Fly Electric Bike, (http://www.gemcar.com)*

These electric bicycleshave 25 km of autonomy, areeasy to park and store - with folding handles - and are non-polluting. The selling price of these innovative electric mini vehicles is between 450 Euro and 1500 Euro, lower than similar products on the European market, which will be an advantage for export. Also here will be produced inclusively the permanent magnet synchronous motors - brushless a. c. motors - that drive these vehicles, in a different range of powers from 200 W to 6 kW.

Numerical Simulations for the Original Configuration of the Permanent Magnet Synchronous Motor

The PMSM - permanent magnet synchronous motor -was studied with the help of numerical modelling and experiments. This is a three-phase synchronous motor with permanent magnets, with which is equipped the electric bicycle in the endowment of the Research Centre - ELECTROMET (http://electromet.upit.ro), where all the experiments were carried out and is having the following rated and constructive data:

- rated power P_n = 500 W;
- rated voltage U_n = 36 V (star connexion on stator);
- rated speed n_n = 130.43 rpm;
- rated frequency f = 50 Hz;
- number of poles pairs p = 23;
- number of stator slots Z_1= 51;
- number of permanent magnets on rotor N_p = 46;
- permanent magnet characteristics: SmCo sintered magnet; relative magnetic permeability μ_r = 1.05; residual magnetic flux density (at 20ºC) B_r = 0.7 T; intensity of the coercive magnetic field (at 20ºC) H_c = 480 kA/m; maximum magnetic energy per volume unit of magnetic material $(BH)_{max}$ = 96 kJ/m^3;
- the permanent magnets in the rotor are radially magnetized;
- the maximum temperature supported by the motor is$T$ = 120 °C;
- ferromagnetic armatures length: 24 mm (rotor) şi 23.5 mm (stator);
- the machine air gap having a width of 1 mm;
- permanent magnet dimensions: length l_m = 24 mm, width b_m = 13 mm, height h_m= 2.5 mm.

In order to reduce the required permanent magnet volume, a magnet of the fourth class, represented by permanent magnets based on rare earths, obtained by sintering, has been selected by means of tests, with medium residual flux densities and very high intensities of coercive magnetic fields and maximum magnetic energies (Krøvel et al., 2004; Ghiţă, 2008).Figure 2 shows a photograph of the motor mounted on the bicycle wheel.

The permanent magnet synchronous motor is delivered in a rim (tire) and is part of the Tucano kit (Spain) with which the electric bicycle is equipped. The modular motor housing facilitates quick and relatively easy disassembly.

Figure 2. *Photograph of the Permanent Magnet Synchronous Motor Mounted on the Bicycle Wheel (Digă, 2015)*

The kit includes the following items related to the bicycle:

- 500 W motor, mounted in the wheel with diameter 627 mm;
- 36 V and 10 Ah Lithium-ion battery with a mass of 2.5 kg;
- Controller;
- Rear package incorporating the controller and battery;
- Pedal assistance system (assisted pedal);
- Brake levers with motor signal cut;
- Light: sensible 7 LEDs;
- Battery and power-on board indicator with power selector;
- Battery charger.

The numerical analysis of the described synchronous motor was based on the 2D/3D model of the electromagnetic field in a stationary magnetic regime, using the finite element method (Digă, 2015).

The numerical modelling of the motor was done by using the professional software FEMM 4.2 (Meeker, Finite Element Method Magnetics) and ANSYS Electromagnetics Low Frequency (ANSYS® RMxprt, ANSYS® Maxwell 2D, ANSYS® Maxwell 3D) from ANSYS Inc. (2008. Ansys-Ansoft 13).

The geometry of the cross-section of the motor has been parameterized, making it easier to modify its various geometric parameters, when it is desired to determine the influence of these parameters on the motor characteristics.

Polar coordinates were chosen for the definition of the cross-section geometry. Discretization of the integration domain was performed in such a way that the density of the elements is smaller onthe outside of the machine and even higher in the area of the air gap, where the magnetic energy density is at itsmaximum. Figure 3 shows the motor discretization mesh across the integration domain,as well asa detail of that mesh, corresponding

to the marked area. It is noted that in the area of the air gap the mesh is denser.

Determining the Magnetic Flux Density Values in a Cross-Section

Starting from the geometry of the cross-section of the model motor and from the characteristics of the material characterizing the motor, the magnetic flux density value is calculated in a cross-section of the motor by using the finite element 2D method. Figure 4 shows the map of the inductive magnetic flux density values, from a cross-section of the motor.

Calculating Some Characteristic Values

Once the magnetic flux density has been calculated from a cross-section of the motor, it is possible to calculate the magnetic fluxes in the various cross-sectional areas using the values of this magnetic flux density, and from here it can be determined the induced electromotive force (emf), during the without and with load operation of the motor, as well as the values of the electric currents flowing through the stator phase windings.

The number of stator slots of the machine is Z_s = 51 and its number of poles is $2p$ = 46. Due to this, the magnetic inductor flux has different values from one pair of poles to another. This is also shown in Figure 5, which shows the spectrum of the inductive magnetic field lines of the motor at any given time. For this reason, this study considered the average value of the inductor magnetic flux Φ on a slot step (at the air gap), the mediation being made for all 51 stator slots of the motor.

The inductor magnetic flux Φ is determined with the equation:

$$\Phi = B \cdot S \qquad (1)$$

where$S$ is the area inwhich this flux is closed and B is the mean value of the magnetic flux density, corresponding to the surface S.This surface can be determined with the following relation:

$$S = t_{zs} \cdot l_s \qquad (2)$$

where$t_{zs}$is the stator tooth step, measured between the axes of two adjacent slots at the machine air gap, and l_s is the axial length of the stator magnetic core(l_s= 23.5 mm). In this case, the stator tooth step is:

$$t_{zs} = \frac{\pi D_s}{Z_s} = 12.25\,\text{mm} \qquad (3)$$

where: D_s – the stator diameter (D_s = 199mm).

Regarding the inductor magnetic flux, defined by the relation (1), it can be said that it corresponds to the magnetic flux corresponding to a stator slot step, and not to the inductor magnetic flux corresponding to a magnetic pole of the motor. It is obvious that maximizing the inductor magnetic flux of a

stator slot step leads to maximizing the polar magnetic flux of the motor. Therefore, it will continue to work with an average magnitude of the magnetic flux of a stator slot step (not with the polar magnetic flux). This is because it is simpler to calculate this flux than to calculate the polar magnetic flux,given thatthe motor has a special stator winding having a number of slots per pole and phase *q*, whose value is given by the relationship:

$$q = \frac{Z_s}{2m_1 p} = \frac{51}{2 \cdot 3 \cdot 23} = 0.3695 \frac{\text{slots}}{\text{pole} \cdot \text{phase}} \quad (4)$$

wherem_1 is the number of phases and p is the number of poles pairs of the motor.

Figure 3. *The 2D Discretization Mesh at the Level of the Air Gap and Stator Slots*

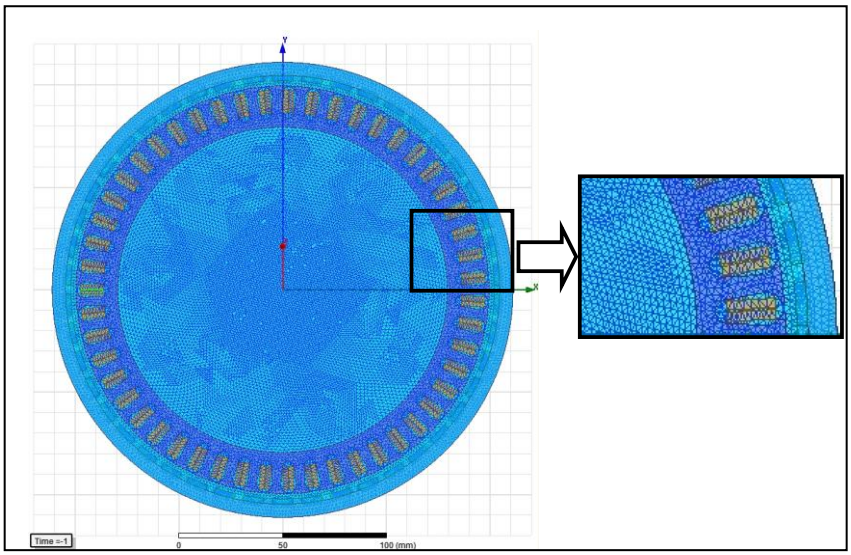

Figure 4. *The Map of the Magnetic Flux Density in a Cross-section of the Motor*

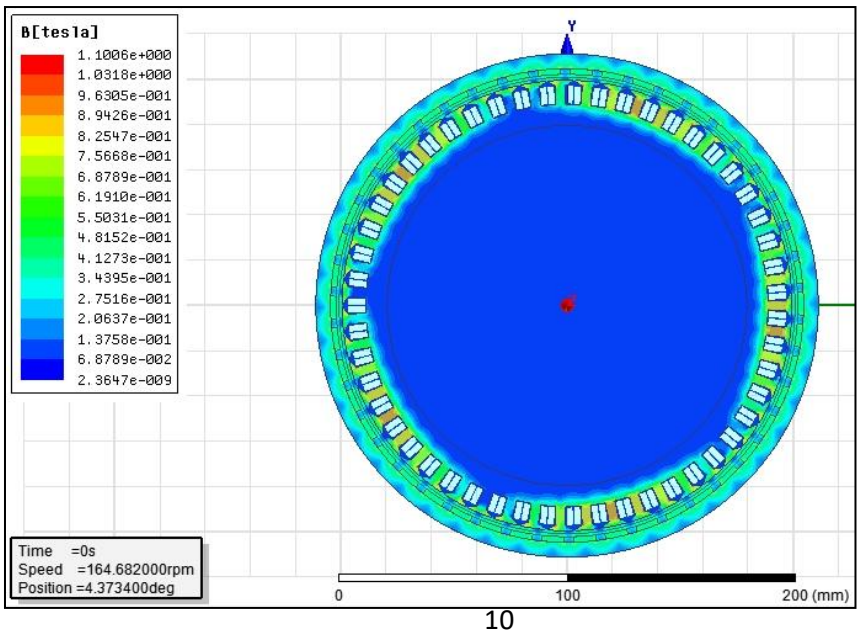

Figure 5. *The Spectrum of the Magnetic Field Lines in a Cross-section*

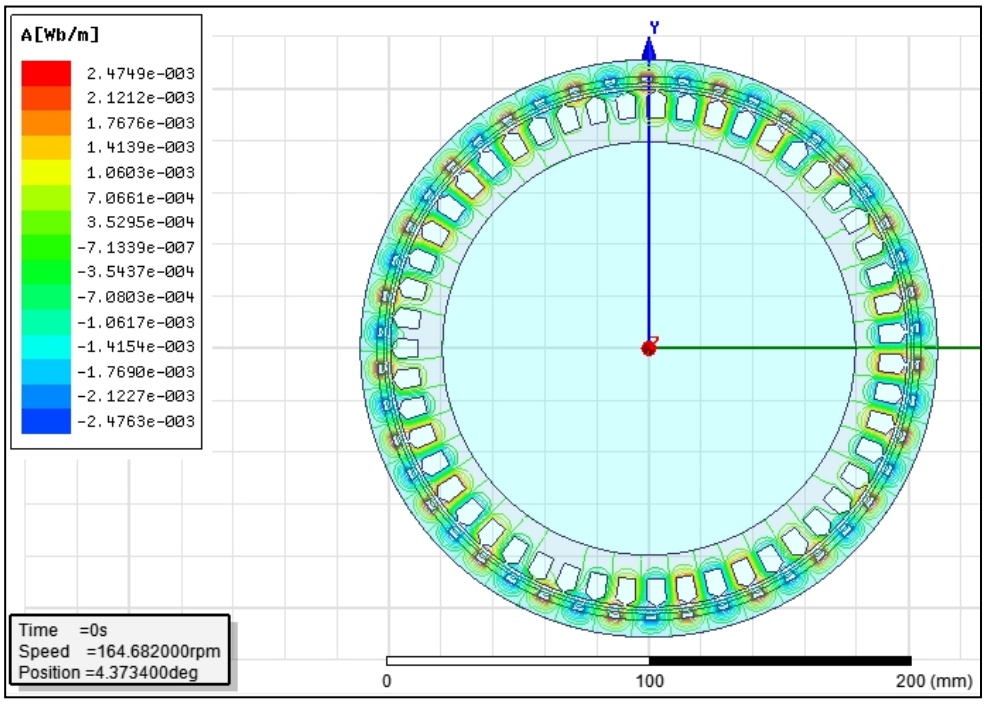

Within the finite element method for studying the inductor magnetic field of the synchronous motor, we should follow the typical steps shown. It is important to emphasize the importance of the way in which the discretization of the computing domain is analyzed, as well as the way in which the results obtained from the application of this method can be analyzed and presentedgraphically (the map of the magnetic flux density, the spectrum of the magnetic field lines in a motor cross-section, the variation of the cogging torque at the initial motor as Maxwell 3D interface, etc.).

Experimental Verifications of the Machine in the Motor Regime

The operating characteristics of the synchronous machine were determined experimentally, both in motor and generator regimes, in the test bench at the University of Piteşti, The Research Centre - ELECTROMET (http://electro met.upit.ro).

In order to carry out experimental verifications of the numerical model in the motor regime, a laboratory installation was made to measure all the necessary quantities, namely: the developed torque, the current absorbed by the motor on each phase, the voltage and the input current in the controller, and the speed of the studied motor. All these measurements were made at different speeds.

Figure 6 and Figure 7 illustrate the assembly. Figure 6 specifically highlights the main components of the mechanical coupling device between the brushless motor (PMSM) and the eddy current disk magnetic brake built to enhance its operating characteristics.

Figure 7 shows a detail of the bicycle driven by the permanent magnet synchronous motor in which the controller and on-board computer are highlighted to show dependence on the particularities (or difficulties) of the route, as well asthe three power levels (ECO, MED, MAX) and motor start. The three power levels of the motor are: 60 % ECO [300 W], 80 % MED [400 W] and 100 % MAX [500 W].

The laboratory assembly, theelectrical scheme of which is shown in Figure 8, contains the following main components:

An adjustable DC Power SupplySource (PS 5005 HQ POWER 0 - 50 VDC / 0 - 5 A) that fed the permanent magnet synchronous motor and generated during the experimental determinations a voltage of 36 V and a current between 0.1 A and 5 A.

An eddy current disk magnetic brake manufacturedby The Research Centre - ELECTROMET and has the possibility to change the rotation angle of its tilting stator. The excitation circuit of the brake may be fed from the c.c. 220 V by means of a rheostat or a controlled rectifier, powered from the c.a. network, in which case the rheostat is removed from the circuit.

A brushless motor (PMSM,) as shownin Figure 6 and Figure 7, is the main motor on which the experimental validations of computations and simulations have been made. This motor was noted as Wheel 1, or the "Big Wheel" of the bicycle (RM) in Figure 8.

A help wheel for driving the brake as shown in Figure 6, has a diameter of 16 cm (the diameter of about 66 cm (rim 26") - the Big Wheel) and moves the shaft which is coupled to the torque transducer. This wheel was marked as Wheel 2, or "Small Wheel" (rm) in Figure 8. The torque transducer is between the small wheel and brake as shown in Figure 6.Its display (display of the torque transducer - HBM HOTTINGER 2555 BALDWIN MESSTECHNIK MVD) is separated.

Figure 6. *The Test Bench for the Experimental Verifications of the Synchronous Motor*

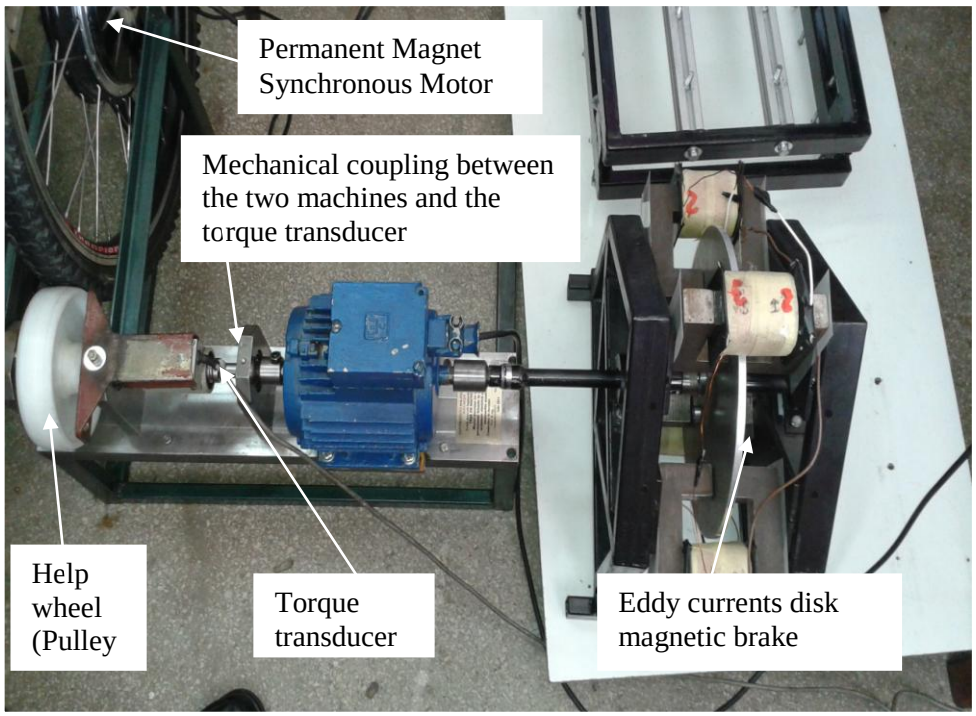

Figure 7. *Detail of the Bicycle driven by the Permanent Magnet Synchronous Motor*

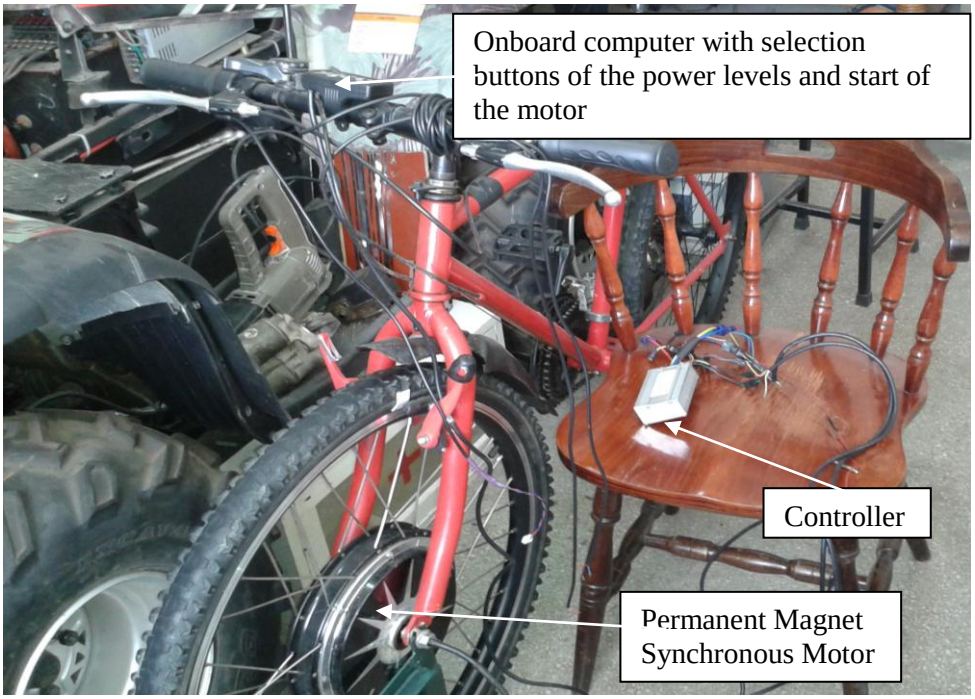

The ammeters A_1, A_2, A_3 indicate the phase current delivered by the controller for the power supply of the brushless motor. The ammeter A_i measures the current delivered by the power supply source. All these ammeters are type Protek 506 DIGITAL MULTIMETER True RMS RS 232C Interface.

The speed was measured by using an electronic tachometer Photo/ Contact TACHOMETER (rpm) Type ebro DT – 2236.

Figure 8 shows the electric scheme for the experimental determination of the mechanical characteristic of the three-phase synchronous motor with permanent magnets studied $M = f(n)$, for $U = U_N$, and a certain value of the angle β of the position transducer ($\beta = 90^0$).

Figure 8. *The Electric Scheme for the Experimental Determination of the Mechanical Characteristic of the Three-phase Permanent Magnet Synchronous Motor*

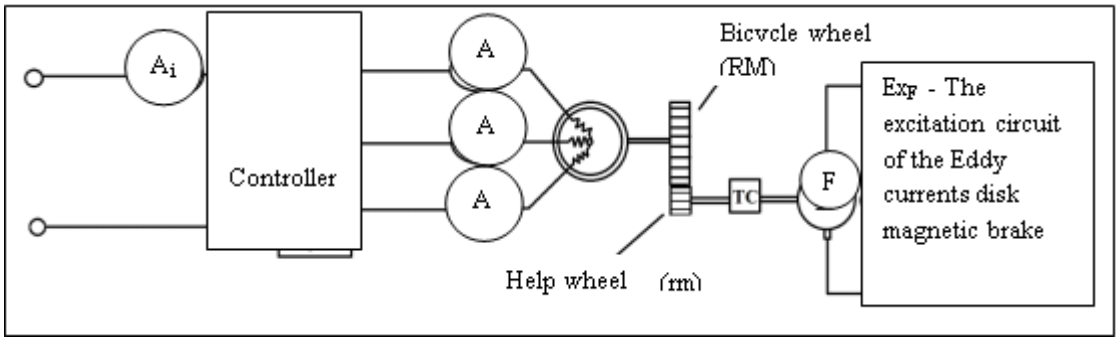

The Mechanical Characteristic: Electromagnetic Torque = f (speed), M = f (n), for U = U_N and a Certain Value of the Position Transducer ($\beta = 90^0$).

The following describes the construction of the calculation algorithm forthe mechanical characteristic M = f (n), for U = $U_{N,}$ which involves the following steps:

- Starting from the relation (5) between the average torque *M* and the speed *n*, used in the advanced simulation techniques with the program "*ANSYS Electromagnetics Low Frequency*" which has the form according to (Nicăet al., 1995; Simion, 1993). Advanced Finite Element Methods (ASEN 5367)) in which the following initial data are entered:

$$M = \frac{k_m \cdot \Phi_0 \cdot \sin\beta}{R}\left(U_f - k_e \cdot \Phi_0 \cdot \sin\beta \cdot n\right) \quad (5)$$

where:

Φ_0– the magnetic flux on the PMSM pole (obtained by calculation or simulation, $\Phi_0 = 2.8788 \cdot 10^{-4}$Wb);
R – the resistance of a stator phase (obtained by calculation or simulation, *R* = 0.5043 Ω);
U_f – the effective value of the phase voltage ($U_N / \sqrt{3} = 36/\sqrt{3} V$);
β – the angle of the time delay of the signals provided by the position transducer of the inverter's semiconductor elements. This angle always shows the command advance, so it is positive.It is set at the initial angle of the transducer $\beta = 90^0$, with the possibility of variance existing in principle.

- The constructive constants k_e, k_m are calculated as solutions of a system of two equations with two unknowns (6), obtained from the condition that the straight line (5) passing through the two points of intersection with the coordinate axes of the characteristic *M = f (n)* obtained by simulation:

$$\begin{cases} M_1 = \left(\frac{k_m \cdot \Phi_0 \cdot \sin\beta}{R}\right) \cdot \left(U_f - k_e \cdot \Phi_0 \cdot \sin\beta \cdot n_1\right) \\ M_2 = \left(\frac{k_m \cdot \Phi_0 \cdot \sin\beta}{R}\right) \cdot \left(U_f - k_e \cdot \Phi_0 \cdot \sin\beta \cdot n_2\right) \end{cases} \quad (6)$$

In this case, we obtained by simulation using the software "*ANSYS Electromagnetics Low Frequency*" the coordinates of the two points: (M_1 = 43.15 Nm, n_1 = 0 rpm) and (M_2 = 0 Nm, n_2 = 200.4 rpm). Thisresults ink_m = $3.637 \cdot 10^3$ and k_e=360.274.

- The mechanical characteristics obtained by calculation and simulation are represented in the same system of coordinate axes, according to Figure 9.

It is observed that during these experimental determinations, the voltage at the motor terminals was kept constant U = U_N, although there are small

variations of this value of maximum ΔU_{ECO} = 5.27 % for the ECO power level and $\Delta U_{MED} = \Delta U_{MAX}$ = 4.72 % for the power levels MED and MAX, respectively.

Therefore, from the mechanical characteristics obtained by calculation and simulation represented in Figure 9, only the portion validated by the measurements was selected.

Thus, in Figure 10 wepresent comparatively the mechanical characteristics electromagnetic torque = f (speed) *M = f (n)*, for U = U_N obtained by: calculation, simulation using ANSYS Maxwell 2D software and measurements carried out for the MAXIM power level, for which the calculation and simulation were performed.

It can be seen that the mechanical characteristic obtained by measurement for the maximum power level has approximately the same slope of - 0.15 Nm/rpm, with the mechanical characteristic obtained by simulation; the torque corresponding to the same speed is higher, with the maximum deviation being 11.668 %.

If we compare this characteristic (the mechanical characteristic obtained by measurement for the maximum power level) with the mechanical characteristic obtained by calculation, it is found that the slope of this characteristic is lower than the slope of the mechanical characteristic obtained by calculation (- 0.15 Nm/rpm < - 0.215 Nm/rpm).

These characteristics have a common point corresponding to the speed of about 190 rpm.Thus,the maximum deviation in absolute value for torque determination is in this case 20.558 %. This point of intersection represents the validation by experimental measurements of the calculations and simulations.

Figure 9. *Comparison between the Mechanical Characteristics Electromagnetic Torque = f (speed)M = f (n), for U = U_N obtained by Calculation (red) and Simulation (blue)*

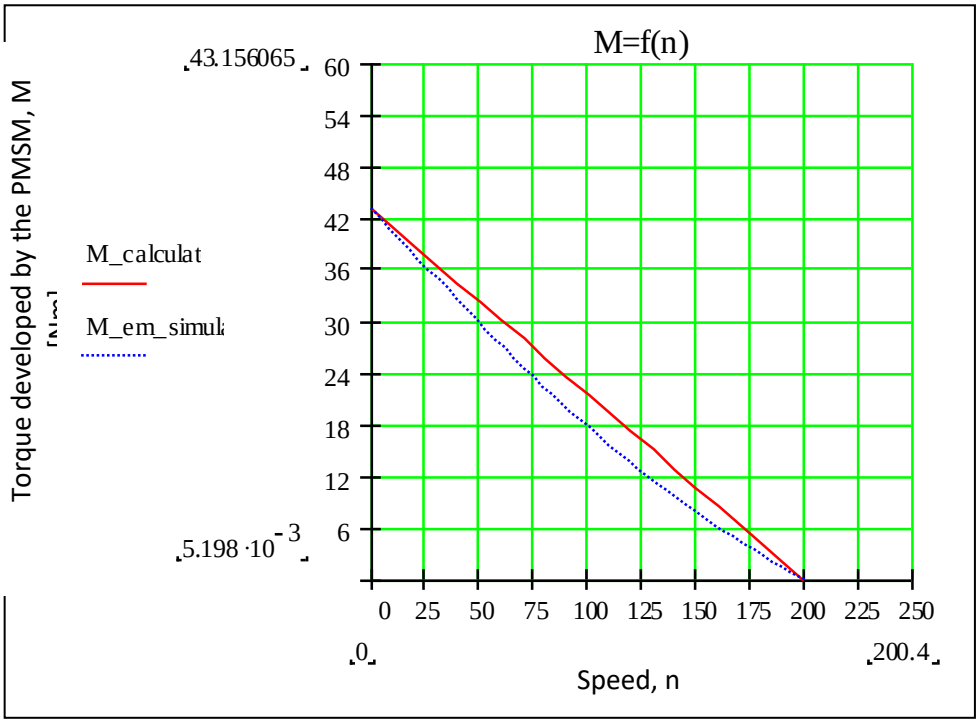

Figure 10.*Comparisonbetween the Mechanical Characteristics obtained by Calculation (red), Simulation (blue) and Measurement (magenta) in a Permanent Regime in the Domain of Reduced Torques*

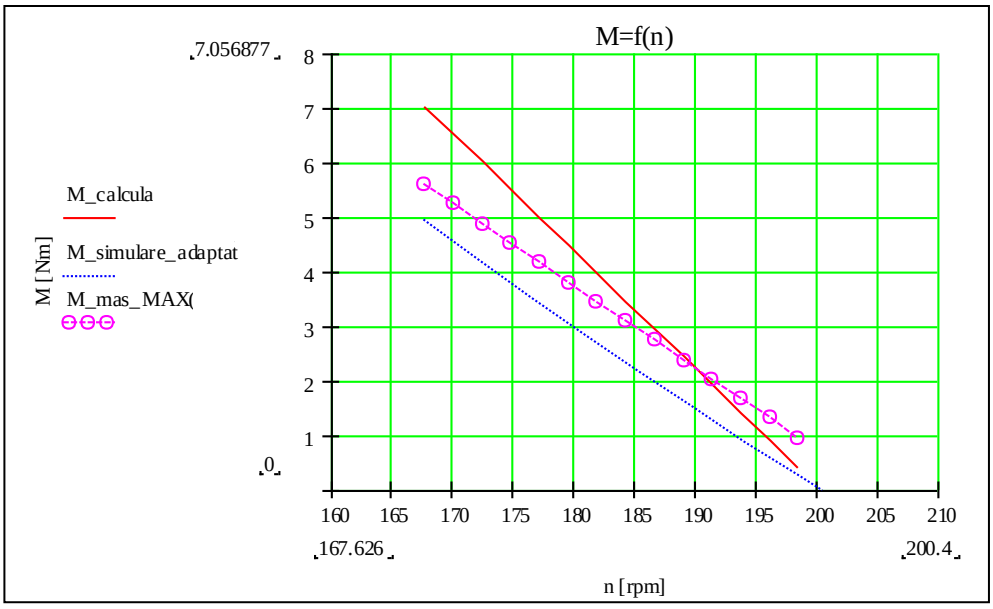

The Characteristic Useful Torque = f (current), M = f (I)

Experimental assembly also allowed raising the characteristic of the useful torque function of the stator current for the studied permanent magnet synchronous motor commanded by the stator.

Thus, in Figure 11 wepresent a comparison of the characteristics of useful torque function of the stator current, obtained by measurement and simulation in a permanent regime for the MAXIM power level, for which the measurements and simulation were performed.

It is thus found that the deviation between these characteristics increases significantly when the current exceeds 14.5 A; the measured torque being higher than the estimated one by simulation with 15.683 %. The slopes of the two characteristics are close as a value, the slope of the characteristic obtained by measurement 0.356 Nm/A being superior to that obtained by simulation 0.30 Nm/A.

The slope of these characteristics, representing the torque per unit of the current at anygiven point, is one of the important quantities that are called to characterize low-power synchronous (permanent magnet) motors as elements of automated systems.

Of the many application areas of permanent magnet synchronous motors, it is worth highlighting a few: electric drives on vehicles and electric traction, etc., are superior to asynchronous motors of the same power (Islam and Husain, 2010; Kisck and Andronescu, 2008). The cost price of the inverter used to supply and command the asynchronous motor is superior to that of the permanent magnet synchronous motor, as it also has to provide the reactive power required for the asynchronous motor operation (Ghiță et al., 2016).

Figure 11. *Comparison betweenthe Characteristics Useful Torque = f (Stator Current) obtained by Measurement (red) and Simulation (blue) in a Permanent Regime, in the Measuring Range allowed by the Test Bench*

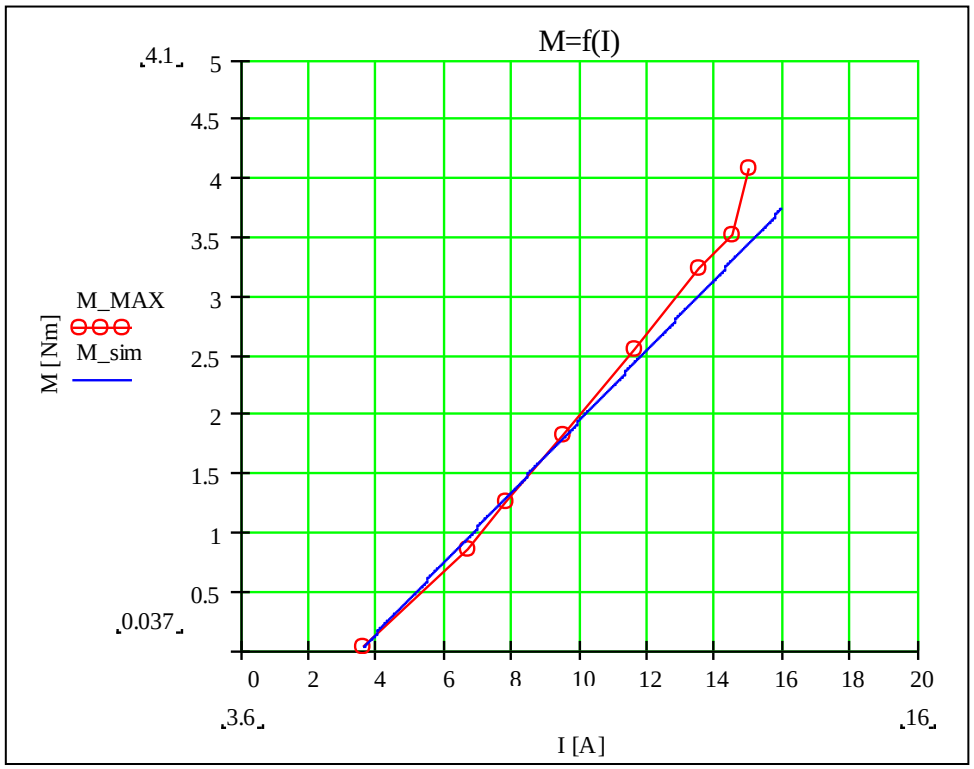

The Characteristic Stator Current = f (speed), $I_f = f(n)$

Experimental assembly also allowed the raising of asecond important operating characteristic of electrical machines with static converters (Sen, 1990), namely *the characteristic stator current = f (speed), $I_f = f(n)$.*

In order to make a comparison between the corresponding characteristics in a permanently measured and calculated regime, some clarifications are required regarding the construction of this characteristic.

The stator current depends on speed, according to Equation 7 below, neglecting the leakage inductance of the stator winding (Sima and Varga, 1986), calculated in (Digă, 2015):

$$I = \frac{1}{\sqrt{3}} \cdot \left(- \frac{k_e \cdot \Phi_0 \cdot \sin \beta \cdot n}{R} + \frac{U_f}{R} \right) \qquad (7)$$

This characteristic necessarily requires that wefollow the prior construction algorithm to compute the mechanical characteristic $M = f(n)$, for $U = U_N$ presented in *Subsection a*, in order to determine the constructive constant k_e.

In Figure 12 and Figure 13 wepresent comparatively the characteristics of the stator current = *f* (speed), $I_f = f(n)$ for $U = U_N$ obtained by calculation and measurements performed for the MAXIM power level.

It should be noted that the test bench allowed us to make determinations only in the second downward part of the stator current characteristic = *f* (speed).

Therefore, for a detailed representation in Figure 13,weselected only this portion of the characteristics stator current = f (speed) where it was also possible to make measurements. In Figure 13, besides the curves obtained by calculation and measurement, the curve obtained by the parabolic two-spline interpolation - *pspline* in Mathcad of the measured values was represented.

Figure 12. *Comparison between the Characteristics Stator Current = f (speed) obtained by Calculation (red) and Measurement (blue) in a Permanent Regime*

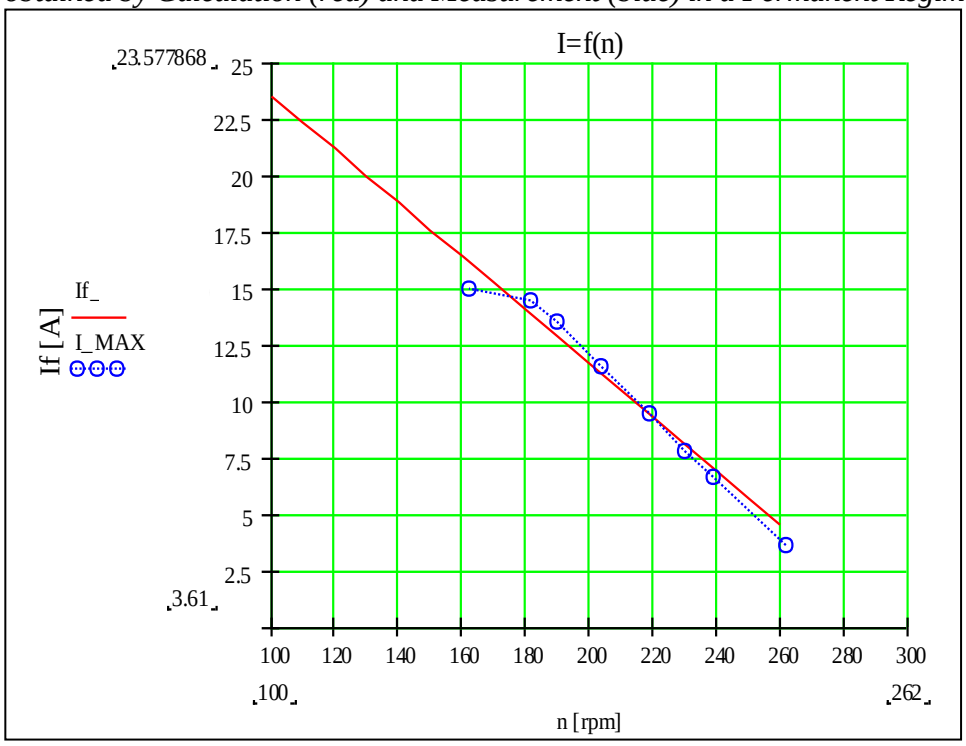

By tests it was concluded that the most appropriate interpolation of these measured values is the one with the function *pspline* compared to the other spline functions (*cspline* - spline function of the third order, cubic or *lspline*- first spline function, linear) and respectively to *linterp* - linear interpolation function.

It is noted that these curves have a common point, corresponding to the speed value of approximately 213 rpm, the maximum deviation of which in the absolute value of the stator current is 4.543 %.

It can also be seen that the slopes of these characteristics are very close in value. The slopes of these characteristics were determined starting from the general equation of the straight, written in the form:

$$ax + by + c = 0 \qquad (8)$$

Figure 13. *Comparison between the Characteristics Stator Current = f (Speed) obtained by Calculation (red), Measurement (blue) and Interpolation of the Measured Values (cyan) in a Permanent Regime in the Measuring Range allowed by the Test Bench*

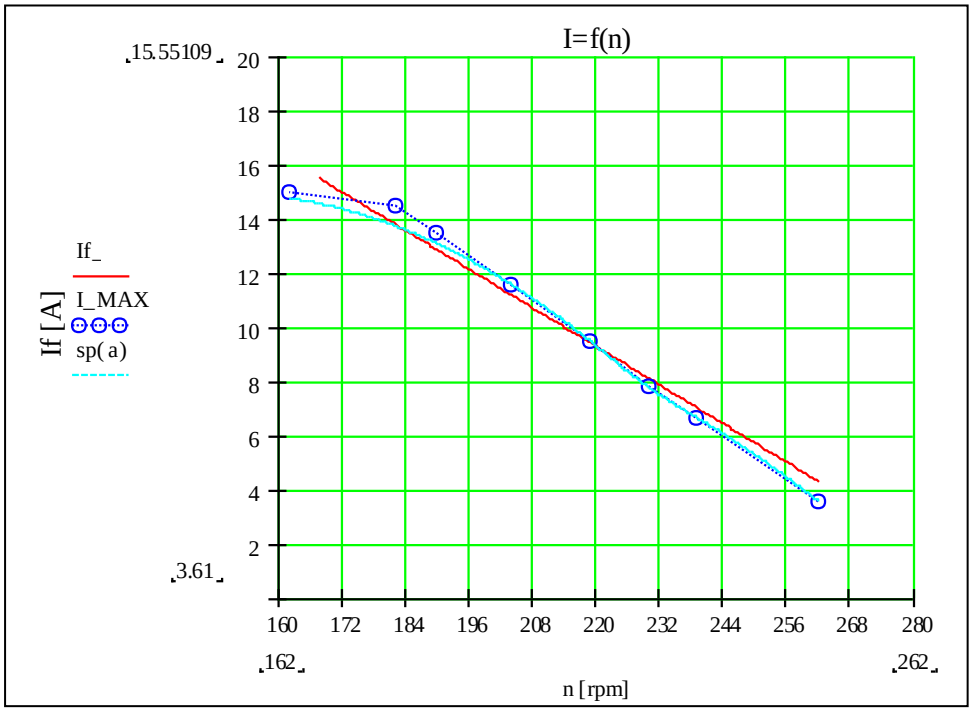

and putting the equation (7) into the form:

$$y = m_d \cdot x + n \tag{9}$$

the resulting slope of the characteristic obtained by calculation is m_d = - 0.119 A/rpm, determined according to the relation (10):

$$m_d = -\frac{a}{b} = -\frac{\frac{k_e \cdot \Phi_0 \cdot \sin\beta}{\sqrt{3} \cdot R}}{1} = -\frac{k_e \cdot \Phi_0 \cdot \sin\beta}{\sqrt{3} \cdot R} \tag{10}$$

The slopes of the characteristics obtained by measurement and interpolation are computed by knowing the coordinates of the two extreme points A, B through which each of them passes:

$$m_{AB} = \frac{y_B - y_A}{x_B - x_A} \tag{11}$$

Thus, it follows that the slope of the characteristics obtained by measurement and interpolation is slightly higher than the slope of the characteristic obtained by calculation: $m_{AB\ MAX}$ = - 0.114 A/rpm >m_d = - 0.119 A/rpm.

Conclusions

The paper deals with a topical issue because the permanent magnet synchronous motors drive systems are growing. In the context of energy efficiency and high reliability requirements, solutions are sought for the development of unconventional urban electric vehicles (scooters, electric bicycles, and electric carts). These require such motors, with low gauges and high reliability, due to the presence of high density energy permanent magnets.

The electric motors used in the drive systems of the electric vehicles are most often chosen to bePermanent Magnet Synchronous Motors. These have the advantage of being safer tooperate without collecting rings or brushes on the rotor. Among their advantages, we can also mention high efficiency and power factor, stable and reliable operation, and lack of additional excitation source of c.c.

To determine the performance characteristics of PMSM, it was necessary to prioritize the useful magnetic flux per pole (obtained by calculation or simulation). The calculations were based on the 2D method of the finite element, the results being useful in the functional-constructive optimization of other synchronous machines with permanent magnets. Numerical investigations were performed by using the Finite Element Method implemented in the FEMM 4.2 and ANSYS® (RMxprt, Maxwell 2D, Maxwell 3D) program packages.

In order to determine the Φ_0 value of the magnetic flux per pole of the PMSM introduced in the relation (5), an analysis concerning the maximisation of the useful magnetic flux of the studied PMSM was made. By maintaining the same diameters of its stator and rotor, this studied the influence of the geometrical parameters of the cross-section of the machine (the stator tooth width, the stator slot opening width, the permanent magnet width, and the height of the stator slot isthmus), as well as the influence of the current density from the stator winding and the ferromagnetic material properties, from which are made the motor stator lamination sheets, on the average magnetic flux corresponding to a stator tooth step of the motor.

Thus, it can be said that the numerical models were validated by experimental verifications of permanent magnet synchronous machines in motor regimes. This was accomplished namely through the measurement of the mechanical characteristic of the motor, of the characteristic of the torque function of the stator current, and of stator current function of the speed. The experimental characteristics were compared with those determined by analytical calculation and a good concordance between them was found.

References

Digă, N., 2015. *Permanent magnet synchronous machines used in electrical bicycles*.Doctoral Thesis. Senate Decision Order Number: 238/30.09.2015. University Politehnica of Bucharest.

ELECTROMET- Research Centre, http://electromet.upit.ro.

Ghiță, C.,2008. *Permanent regimes of electromechanical converters*. MATRIX ROM Publishing House Bucharest. (In Romanian).

Ghiță, C., Digă, N., Constantin, D., Vlad, I. and Digă, S. M., 2016.Finite Element Analysis of the Useful Magnetic Flux of a Low Speed PMSM, In *University POLITEHNICA of Bucharest Scientific Bulletin*, Series C, Vol. 78, Iss.1, 2016, p. 187-198, ISSN 2286-3540.

Islam, R. and Husain, I. 2010. Analitical Model for Predicting Noise and Vibration in Permanent-Magnet Synchronous Motors. In Industry Applications, *IEEE Transactions* on, vol. 46, no. 6, p. 2346-2354, Nov.-Dec. 2010, doi: 10.1109/TIA.2010.2070473.

Kisck, D. O. and Andronescu, Gh. 2008. *Propulsion systems for electric vehicles*. Vol II. Electra Publishing House Bucharest. (In Romanian).

Krøvel, Ø., Nilssen, R., and Nysveen, A. 2004. *A Study of the Research Activity in the Nordic Countries on Large Permanent Magnet Synchronous Machines.* NORPIE 2004.

Meeker, D.,Finite Element Method Magnetics, http://bit.ly/2rBBwUL.

Nică, C., Busuioc, Şt., and Enache, S. 1995. *Electric Micromachines. Laboratory guide*. University of Craiova. Faculty of Electromechanics. Reprography of the University of Craiova.(In Romanian).

Sen, P. C. 1990. Electric Motor Drives and Control – Past, Present and Future, In *IEEE IE*, vol. IE 37, No. 6, December 1990, pp. 562-575.

Sima, V., and Varga, A. 1986.*The practice of computer-aided optimization*.Technical Publishing House Bucharest.(In Romanian).

Simion, Al., 1993. *Special electrical machines for automation*. Universitas Publishing House Chisinau.(In Romanian).

*** http://www.gemcar.com.

*** 2006. Advanced Finite Element Methods (ASEN 5367) - Spring 2006, Aerospace Engineering Sciences - University of Colorado at Boulder - http://bit.ly/2DH9GLA.

*** 2008. Ansys-Ansoft 13, User' guide, ansoft-corporation.software.informer.com.

*** https://e-twow.ro.